The Sixth International Workshop on Micro and Nanotechnology for
Power Generation and Energy Conversion Applications, Nov. 29 - Dec. 1, 2006, Berkeley, U.S.A.

Analysis of Annular Seals for High-Speed Power-MEMS Devices

C. J. Teo* and Z. S. Spakovszky

Gas Turbine Laboratory, Massachusetts Institute of Technology
77 Massachusetts Av., Cambridge, MA02139, U.S.A.

Abstract

High-speed rotating power-MEMS devices often require annular seals to isolate turbomachinery and gas bearing components that operate at different static pressure settings. Rotordynamic instability may arise due to dynamic coupling effects between the annular seals and other integral components of the micro-power system. Design guidelines to avoid such instabilities have been established and applied in the redesign of a MEMS air-turbine, enabling a measured maximum rotor speed of 1.7 million rpm and a rotor tip velocity of 370 m/s.

Keywords: Power-MEMS, Micro-gas turbine, Micro-gas bearing, Annular seals

1 – INTRODUCTION AND BACKGROUND

One of the goals of the MIT Microengine Project is to develop high-speed rotating power-MEMS devices with power densities significantly higher than their macro-scale counterparts [1]. The rotating micro-machinery must be operated at rotor tip velocities of order 300-500 m/s to achieve the target levels of power density. The MIT power-MEMS devices share a common bearing technology which is tested in a gas-bearing supported MEMS air turbine depicted in Figure 1. The high speed rotors, whose design speed is of order 2 million rpm, are supported radially and axially by hydrostatic gas journal and gas thrust bearings, respectively.

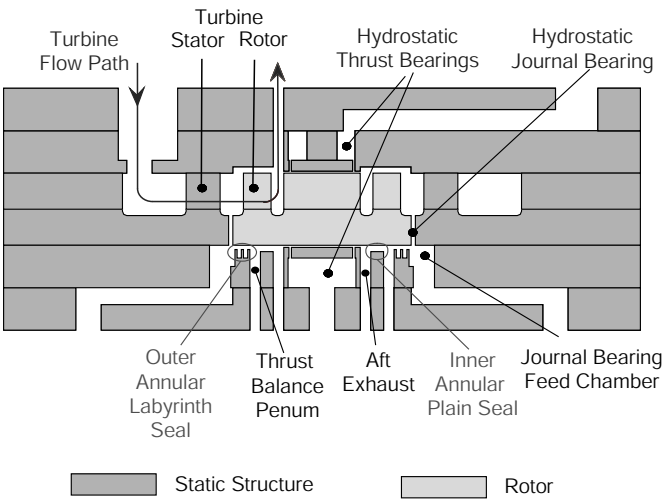

Figure 1 – Cross sectional view of the gas-bearing supported MEMS-air turbine (not to scale).

Such power-MEMS devices consist of closely coupled turbomachinery and gas-bearing components. To enable the operation of the components at different static pressure settings, annular seals are required. On the aft side of the rotor shown in Figure 1, an inner plain seal separates the aft exhaust from the thrust balance plenum, which is in turn isolated from the journal bearing feed chambers by an outer labyrinth seal consisting of row of annular teeth and grooves. Unlike in stationary devices, static or dynamic instability may arise due to rotordynamic coupling between the annular seal flows and other integral components of the power-MEMS device. A key challenge in the design of such seals is to ensure that the leakage flows do not deteriorate the performance and the dynamic stability of the high-speed gas bearings.

2 – CHALLENGES AND NATURE OF THE ISSUES

Practical design solutions and guidelines are proposed based on two different types of destabilizing negative stiffness effects that were identified in previous experimental work.

2.1 – Negative Radial Stiffness

As illustrated in Figure 2(a), the hydrostatic flow to the journal bearing is supplied axially via feed chambers on the aft side of the rotor. In earlier designs of this MEMS air-turbine, circumferential portions of the journal bearing were blocked off from the feed chambers via annular seals, as shown in Figure 2(b). The rationale for such an arrangement is to introduce anisotropy in journal bearing stiffness to enhance bearing dynamic stability and to relieve the stringent microfabrication tolerance requirements [2]. Under normal operating conditions, the static pressure difference between the exit of the journal bearing and the annular seal in the blocked region drives a leakage flow from the turbine side into the journal bearing through the annular seal towards the balance plenum.

Figures 2(b) and 2(c) illustrate schematically how a negative radial stiffness is generated due to this leakage flow. The crux

* Contact author: Tel: 617-253-3732, email: teocj@mit.edu

of the matter is that the reverse flow through the journal bearing occurs in series with the flow through the annular seal. Figure 2(b) shows a radially-centered rotor with no net radial force acting on the rotor, and a nominal overall static pressure difference of 5 psi across the journal bearing and seal. However, when the rotor is deflected by a small radial perturbation, as shown in Figure 2(c), the pressure drop or hydraulic loss across the journal increases over the region of reduced journal bearing clearance and decreases over the enlarged clearance on the opposite side. This yields a higher average static pressure in the bearing land on the enlarged clearance side and reduces the average pressure on the opposite side. Thus a net radial force acts in the direction of rotor displacement inducing a destabilizing negative stiffness. It is evident that the cause of this negative radial stiffness is due to the coupling of the flow through the journal bearing and the annular seal.

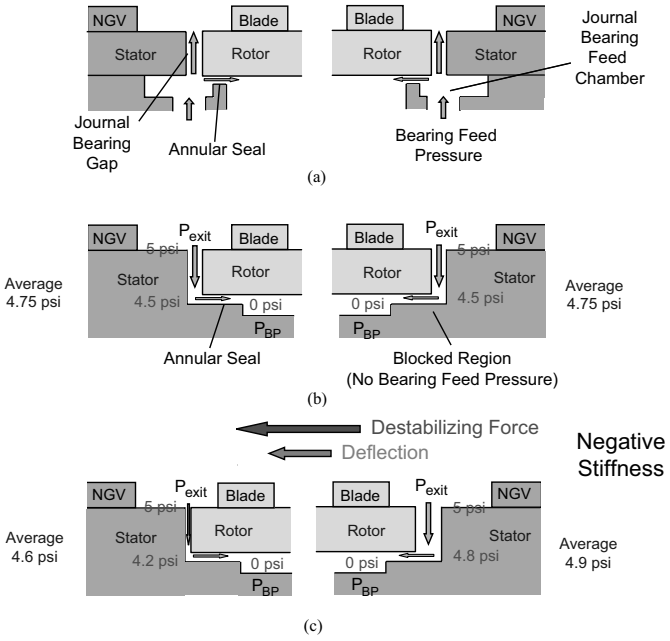

Figure 2 – (a) Journal bearing flow in unblocked region. (b) and (c) Mechanism for negative (destabilizing) radial stiffness due to coupling of reverse flow through journal bearing land and annular seal in blocked region.

The key implication of the above analysis is that in order to avoid any undesirable negative radial stiffness due to reverse flow through the journal, the flow resistance in the journal bearing land must not be directly connected in series with any other hydraulic resistance.

2.2 – Negative Tilting Stiffness

The other type of negative stiffness previously encountered in a MEMS-Electrostatic-Turbine-Generator is a negative tilting stiffness arising from the radially inward flow through an annular seal as shown hatched on the bottom of Figure 3. When the rotor is subjected to a small tilting perturbation about its equilibrium position, a radially and circumferentially varying gap is formed between the balance plenum and the aft exhaust. Since the hydraulic resistance at any location scales inversely with the cube of the local gap or clearance, a rotor tilt is anticipated to give rise to a static pressure distribution with a strong axial gap dependency. Figure 3 on the top depicts a typical static pressure distribution over the annular seal that separates the balance plenum from the aft-exhaust. The calculation was obtained using a finite-element method and corresponds to a rotor tilting angle of -0.0006 radians equivalent to a rotor tip deflection of 1.3 μm. The nominal seal clearance in the absence of any rotor tilt is 3 μm. The supply pressure to the balance plenum is fixed at 5 psig, and the aft exhaust is vented to ambient atmospheric conditions. The tilting causes a reduction in axial gap over the left-half portion of the seal, and an increase over the right-half portion. Regions of increased hydraulic resistance (reduced static pressure) have thus shifted towards the balance plenum inlet along the left-half portion, whereas regions of reduced hydraulic resistance (increased static pressure) have shifted towards the balance plenum inlet along the right-half portion. The redistribution in static pressure over the annular seal causes a net rolling or pitching torque acting on the rotor. This torque is destabilizing because it acts in the direction of rotor tilt further increasing the rotor tilting angle.

The magnitude of the negative tilting stiffness increases monotonically with decreasing seal clearances. This becomes a challenging issue in MEMS-electrostatic-turbine-generators, where small seal clearances are necessary to generate the required power levels. Experiments were performed on a MEMS-electrostatic-turbine-generator with a nominal seal clearance of 3 μm. At a maximum rotor speed of 850,000 rpm, the pressure difference across the seal was 5 psi. This corresponds to a destabilizing negative stiffness of 0.03 N-m/rad, which is approximately equal in magnitude to the thrust bearing tilting stiffness [3]. The rotor failed at the said speed most likely due to the negative tilting stiffness arising from the radially inward flow through the annular seal.

Labyrinth seals can significantly reduce the negative stiffness arising in situations where a variable resistance, such as the flow resistance through a bearing land, is coupled in series with the hydraulic resistance of a seal. Such seals consist of a row of teeth and grooves (or slots) which have negligible hydraulic resistance in the circumferential direction as compared to the teeth, and serve to mitigate possible circumferential static pressure non-uniformities. Thus any possible net torque, and as a consequence a destabilizing tilting stiffness experienced by the rotor, can be appreciably reduced.

3 – ANALYTICAL ANNULAR SEAL MODEL

In view of the low Reynolds numbers and high pressure ratios across the seals, compressibility effects have to be taken into account to accurately estimate the flow characteristics of

annular seals. A compressible flow model based on the method of influence coefficients was developed to characterize the steady-state behavior of annular labyrinth seals in power-MEMS devices. The main objective of the model is to quantify the dependence of the leakage mass flow on seal clearance distribution and static pressure ratio. The analytical fluid resistance model accounts for drops in stagnation pressure due to seal inlet losses and viscous losses over the seal face.

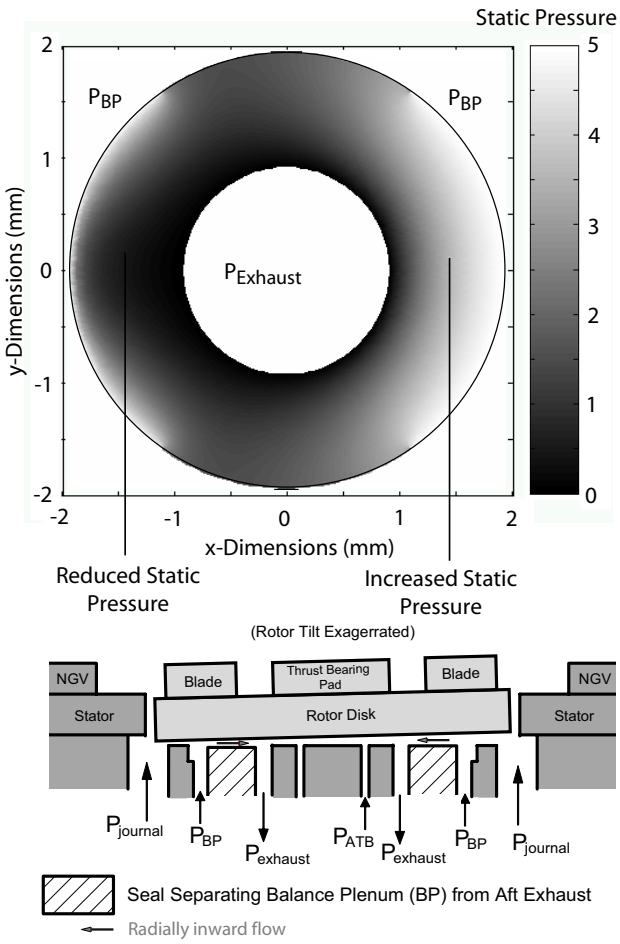

Figure 3 – Annular seal static pressure distribution for a rotor tilting angle of -0.0006 radians equivalent to a rotor tip deflection of 1.3 μm.

The inlet stagnation pressure loss at the entrance to the teeth of the labyrinth seal is described by

$$\frac{\Delta P_t}{P_t - P} = 0.5 \,. \tag{1}$$

The quasi one-dimensional, viscous, compressible flow through each tooth is then computed using influence coefficients for effects of friction, heat addition and flow area change [4]. In view of the high thermal conductivity of silicon, the flow through the teeth is assumed to be isothermal. Final analytical expressions (detailed derivations are given in [5]) for fractional changes in the square of Mach number, dM^2/M^2, and static pressure, dP/P, due to a change in radial location dr across the annular seal are given by

$$\frac{dM^2}{M^2} = -\left[\frac{2\left(1+\frac{\gamma-1}{2}M^2\right)}{1-M^2} + \frac{(\gamma-1)M^2\left(1+\gamma M^2\right)}{\left(1-M^2\right)\left(1-\gamma M^2\right)}\right]\frac{dr}{r}$$

$$+\left[\frac{\gamma(\gamma-1)M^2\left(1+\gamma M^2\right)}{2\left(1-M^2\right)\left(1-\gamma M^2\right)} + \frac{\gamma M^2\left(1+\frac{\gamma-1}{2}M^2\right)}{1-M^2}\right]\frac{48\mu\pi r}{\dot{m}h}dr \,, \tag{2}$$

and

$$\frac{dP}{P} = \left[\frac{\gamma M^2}{1-M^2} + \frac{\gamma(\gamma-1)M^4}{\left(1-M^2\right)\left(1-\gamma M^2\right)}\right]\frac{dr}{r}$$

$$+\left[-\frac{\gamma^2(\gamma-1)M^6}{2\left(1-M^2\right)\left(1-\gamma M^2\right)} - \frac{\gamma M^2\left(1+(\gamma-1)M^2\right)}{2\left(1-M^2\right)}\right]\frac{48\mu\pi r}{\dot{m}h}dr \,. \tag{3}$$

In Equations (2) and (3), $\dot{m}$ denotes the mass flow through the seal of clearance h, whereas μ and γ represent the dynamic viscosity and the ratio of specific heats of the fluid. The above two equations are used to numerically compute the fractional changes in the Mach number and static pressure across the entire tooth width. In view of the significantly larger depths of the grooves as compared to the teeth, the static pressure along each groove can be assumed constant, implying that the radial and circumferential hydraulic resistances in the grooves are negligible. In addition, the flow is assumed to lose all of its dynamic head when exiting a tooth and venting into a groove. For a specified seal clearance, together with prescribed seal inlet and exit static pressure boundary conditions, the required mass flow rate through the seal is then obtained numerically.

The developed analytical model was used to assess the as-fabricated clearance of an annular seal by quantifying the leakage mass flow for different seal pressure ratios. In addition, the analytical model was successfully applied to determine the rotor axial position during high-speed operation of micro-devices. Knowledge of the rotor axial position is crucial, as it is necessary to axially center the rotor between the forward and aft thrust bearings to avoid physical contact between the rotor and static structure.

Figure 4 compares experimental measurements and model predictions of the corrected seal mass flow as a function of static pressure ratio across the labyrinth seal of a MEMS-turbopump for a given seal clearance. In contrast to an incompressible flow model, the results of the fully compressible flow analysis are in good agreement with the experimental measurements, confirming the importance of modeling compressibility effects. The analytical model was subsequently employed to determine the rotor axial position during actual high-speed testing of the same device.

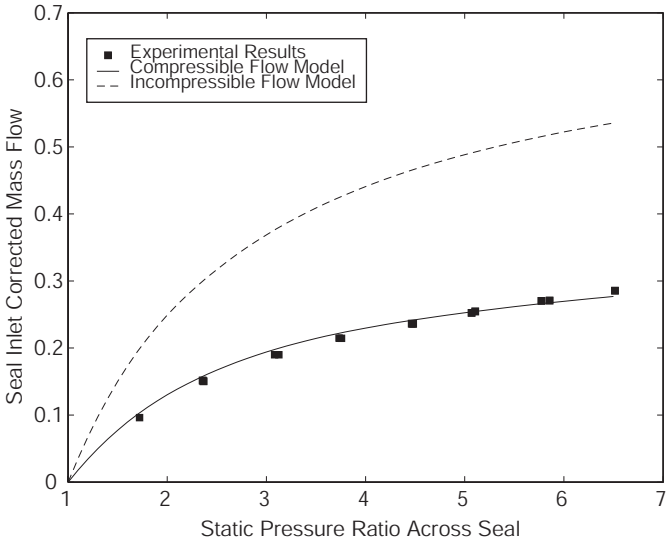

Figure 4 – Experimental measurements and model predictions of seal inlet corrected mass flow for various labyrinth seal static pressure ratios in a MEMS-turbopump.

4 – APPLICATION AND SYNTHESIS

The annular seals in the new generation MEMS air-turbine depicted in Figure 1 were redesigned based on the above model. The redesign synthesized the lessons learnt and insight gained from previous experimental and analytical work. The dynamic coupling illustrated in Figures 2(b) and 2(c) was eliminated by implementing a four-chamber journal bearing feed system. An outer labyrinth seal was adopted to reduce the negative tilting stiffness.

Controlled high speed operation up to 70% of design speed was demonstrated. This corresponds to a rotor rotation rate of 1.7 million rpm, a rotor tip velocity of 370 m/s and a bearing *DN* number of 7 million mm-rpm. Moreover, repeatable high-speed stable gas bearing operation above 1 million rpm was successfully demonstrated in a large number of devices. The operating schedule adopted for two new generation MEMS air-turbines is presented in Figure 5. Also shown in the same figure is the operating schedule for a previous-generation MEMS air-turbine (marked in grey). The redesigned MEMS air-turbines are capable of achieving speeds approximately double of those reached by previous-generation MEMS air turbines and yield improved operability as indicated by only three to four necessary adjustments in journal bearing feed pressure as compared to over twenty required in the past.

The in-depth analysis and redesign of the annular seals were one of the crucial enablers of repeatable, stable high-speed operation of MEMS air-turbines, demonstrating the feasibility of micro-scale turbomachinery.

5 – CONCLUSIONS

Causes of rotordynamic instability in annular seals were identified and engineering solutions and design guidelines were established to alleviate negative radial and tilting stiffness. The solutions and guidelines were applied in the design of a MEMS air-turbine, which demonstrated a rotor rotation rate of 1.7 million rpm and a rotor tip velocity of 370 m/s.

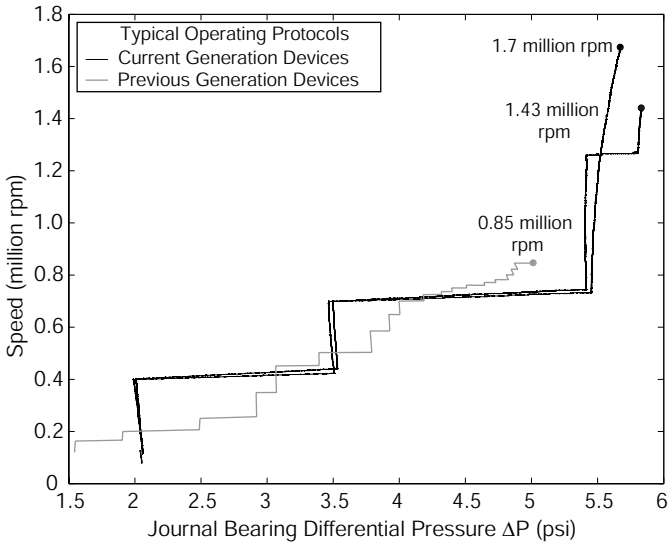

Figure 5 – Comparison of typical operating protocols for previous and current generation MEMS air-turbines. Maximum rotor speed for current generation devices is 1.7 million rpm.

ACKNOWLEDGEMENTS

The authors would like to thank Dr. F. F. Ehrich, Dr. S. A. Jacobson and Dr. L. X. Liu for their very useful discussions and helpful comments, and Dr. H. Q. Li and L. C. Ho for their invaluable help and insight into micro-fabrication issues. This research was sponsored by the US Army Research Laboratory under the Power and Energy Collaborative Technology Alliance Program.

REFERENCES

[1] Epstein, A. H. and Senturia, S. D., "Macro Power from Micro Machinery," *Science*, Vol. 276, pp. 1211, May 1997.

[2] Liu, L. X., "Theory for Hydrostatic Gas Journal Bearings for Micro-Electro-Mechanical Systems," MIT PhD Thesis, September 2005.

[3] Teo, C. J. and Spakovszky, Z. S., "Analysis of Tilting Effects and Geometric Non-uniformities in Micro-Hydrostatic Gas Thrust Bearings," *ASME J. of Turbomachinery*, Vol. 128, pp. 606-615, October 2006.

[4] Shapiro, A. H., "The Dynamics and Thermodynamics of Compressible Fluid Flow, Vol. I," New York: Ronald Press, 1953.

[5] Teo, C. J., "MEMS Turbomachinery Rotordynamics: Modeling, Design and Testing," MIT PhD Thesis, June 2006.